Influence of elastic strain gradient on the upper limit of flexocoupling strength, spatially modulated phases, and soft phonon dispersion in ferroics

Anna N. Morozovska,[1,2,*] Eugene A. Eliseev,[3] Christian M. Scherbakov,[2] and Yulian M. Vysochanskii[4,†]

[1]*Institute of Physics, National Academy of Sciences of Ukraine, 46, Prospekt Nauky, 03028 Kyiv, Ukraine*

[2]*Taras Shevchenko Kiev National University, Physical Faculty, Chair of Theoretical Physics, 4e, pr. Akademika Hlushkova, 03022 Kyiv, Ukraine*

[3]*I. Frantsevich Institute for Problems of Materials Science, National Academy of Sciences of Ukraine, 3, Krizanovskogo, 03142 Kyiv, Ukraine*

[4]*Institute of Solid State Physics and Chemistry, Uzhgorod University, 88000 Uzhgorod, Ukraine*

(Received 7 June 2016; revised manuscript received 1 October 2016; published 21 November 2016)

Using the Landau-Ginzburg-Devonshire theory, we established the role of the flexoelectric coupling between the gradients of elastic strain and polarization in the stability of spatially modulated phases in ferroics, such as incipient and proper ferroelectrics with commensurate and incommensurate long-range-ordered phases. We included the square of elastic strain gradient in the Landau-Ginzburg-Devonshire functional because this term provides the functional stability for all values of the strain gradient. Analytical expressions for polarization, strain, dielectric susceptibility, and stability threshold were derived for a one-dimensional case. The expressions show that the maximal possible values of the static flexoelectric effect coefficients (upper limits) established by Yudin, Ahluwalia, and Tagantsev without the square of elastic strain gradient and other higher order gradients terms lose their direct meaning. Considering the gradients, the temperature dependent condition for the flexocoupling magnitude exists instead of the upper limits. Also, we established that spatially modulated phases appear and become stable in commensurate ferroelectrics if the flexocoupling constant exceeds a critical value. The critical value depends on the electrostriction and elastic constants, temperature, and gradient coefficients in the Landau-Ginzburg-Devonshire functional. We calculated soft phonon dispersion in commensurate and incommensurate long-range-ordered phases of ferroelectrics with the square of elastic strain gradient, static, and dynamic flexocoupling. It appeared that the dispersion of the optical mode is slightly sensitive to the flexocoupling, and the dispersion of acoustic mode strongly depends on the coupling magnitude. Obtained results demonstrate that nontrivial differences in the dispersion of optical and acoustic modes occur with the change of flexocoupling constant. Therefore, experimental determination of soft phonon dispersion might be very informative to study the influence of strain gradients and flexocoupling on the spatially modulated phase in ferroelectrics with commensurate and incommensurate long-range order.

DOI: 10.1103/PhysRevB.94.174112

I. INTRODUCTION

The static flexoelectric effect is the appearance of electric polarization in solids as response to the strain gradient and vice versa [1]. The effect was first predicted from microscopic consideration by Mashkevich and Tolpygo [2], and shortly after the link to the continuous medium formalism was established by Kogan [3]. According to the continuous medium approach, the polarization component variation δP_i induced by the static flexoelectric effect is linearly proportional to elastic strain gradient components, $\partial u_{ij}/\partial x$, and the proportionality coefficient is the component of the flexocoupling tensor f_{ijkl}, $\delta P_i = f_{ijkl}\frac{\partial u_{kl}}{\partial x_j}$. Following Kogan [3], f_{ijkl} values are quite small, $|f_{ijkl}| \sim e/a$, where e is the electron charge and a is the lattice constant. The dynamic flexoelectric effect considered microscopically by Axe *et al.* [4] and phenomenologically by Yudin and Tagantsev [5] and Kvasov and Tagantsev [6] contributes to the polarization variation, $\delta P_i = -\frac{M_{ij}}{\alpha}\frac{\partial^2 U_j}{\partial t^2}$, where U_j are the components of elastic displacement, M_{ij} are the components of flexodynamic tensor, and α is the dielectric stiffness. The dynamic flexoelectric effect corresponds to the polarization response to accelerated motion of the medium in the time domain.

Flexoelectricity occurs in all 32 crystalline point groups because the strain gradient breaks the inversion symmetry. Owing to the universal nature, flexoelectricity permanently attracts broad scientific interest [5,7], but its application potential in homogeneous macroscopic materials is fundamentally limited due to the small f values.

In contrast to homogeneous macroscopic systems, it is difficult to estimate the significance of the flexoelectric phenomena in ferroics and multiferroics (e.g., antiferroelectrics, ferrielectrics, ferroelectrics, superparaelectrics, and magnetoelectrics) [8–10], which are either nanosized (e.g., thin films, nanoparticles, fine-grained ceramics) or possess nanoscale heterogeneity [e.g., nanoregions, dense nanodomain structures, spatially modulated phases (SMPs)] of the order parameter (e.g., spontaneous polarization, magnetization, antiferromagnetic order parameter) [11]. The gradient of the order parameter interacts with elastic strains in nanostructured ferroics via the flexocoupling (e.g., flexoelectric, flexoantiferrodistortive, or flexomagnetic couplings). Hence the flexocouplings strongly change the structural, polar, and electrotransport properties of ferroic thin films [12–15], nanoparticles [16,17], fine-grained ceramics [18,19], ferroelectric [20–23], and ferroelastic [24,25] domain walls and interfaces as well

*anna.n.morozovska@gmail.com

†vysochanskii@gmail.com

as inducing reentrant phases [26] and incommensurate SMPs [27–29] in ferroelectrics.

Considering the importance of the flexoelectricity for the physical understanding of mesoscale and nanoscale couplings in ferroelectrics, one has to determine the static (f_{ijkl}) and dynamic (M_{ij}) coupling constants. It appeared that the values f_{ijkl} calculated from the first principles [30–33] according to Kogan's microscopic definition [3] can be several orders of magnitude smaller than those measured experimentally [34–36]. The discrepancy motivated Yudin, Ahluwalia, and Tagantsev to establish theoretically the upper limits for the values of the static flexoelectric coefficients f_{ijkl} in ferroelectrics [37]. The calculated maximal values of f_{ijkl} showed that the anomalously high flexoelectric coefficients measured for perovskite ceramics [34–36] cannot be related with the manifestation of the static flexoelectric effect.

Note that Yudin, Ahluwalia, and Tagantsev used the Landau-Ginzburg-Devonshire (LGD) free energy, which included the flexoelectric term in the form of the Lifshitz invariant $\frac{f_{ijkl}}{2}(P_i\frac{\partial u_{kl}}{\partial x_j} - u_{kl}\frac{\partial P_i}{\partial x_j})$ [1,5,37,38] but did not include the quadratic term of elastic strain gradient $\frac{v_{ijklmn}}{2}(\frac{\partial u_{ij}}{\partial x_m}\frac{\partial u_{kl}}{\partial x_n})$. The gradient term is omitted in the free energy of ferroics considered in most studies, with the exception of several papers, e.g., Eliseev *et al.* [16], Yurkov [39], Mao and Purohit [40], and Stengel [41].

Note that Eliseev *et al.* [16] pointed out that the square of elastic strain gradient creates the stable smooth distribution of the order parameter for all values of the strain gradients since the presence of the Lifshitz invariant essentially changes the stability conditions of the LGD free energy. Eliseev *et al.* [16] stated that the term $\frac{v_{ijklmn}}{2}(\frac{\partial u_{ij}}{\partial x_m}\frac{\partial u_{kl}}{\partial x_n})$ can be neglected only for small strain gradients under the condition $f^2_{klmn} < g_{ijkl}c_{ijmn}$, wherein c_{ijmn} are the components of elastic stiffness tensor and g_{ijkl} are the components of polarization gradient tensor. Yurkov [39] demonstrated that the square of elastic strain gradient changes the existing boundary conditions for polarization and strains and produces the new form of elastic boundary conditions. Mao and Purohit [40] propose a general formalism for a flexoelectric phenomena description in linear anisotropic dielectrics. They included the quadratic contribution of the strain gradient tensor in the free energy functional but ignored the quadratic term of the electric polarization gradient $\frac{g_{ijkl}}{2}(\frac{\partial P_i}{\partial x_j}\frac{\partial P_k}{\partial x_l})$ and did not consider a ferroelectric nonlinearity. The role of the strain gradient can be established from the analytical solutions obtained by Mao and Purohit [40] for a number of practically important geometries. Stengel [41] evolved the *ab initio* approach for determination of the flexocoupling tensor. He considered soft phonon spectra calculated from the first principles and pointed out the gradient of elastic strain effects on the spectra. Also, Stengel [41] discussed the qualitative conditions of the free energy functional stability.

Let us emphasize that basic experimental methods, which contain information about the spatial modulation of the order parameter in ferroics (such as antiferroelectrics, proper, and incipient ferroelectrics), are dielectric measurements [42], inelastic neutron scattering [4,43–48], x-ray [49–52], Raman [53], and Brillouin [49,52,54] scattering. Theoretical analysis of the flexocoupling contribution to the soft phonon eigenvectors revealed that if the stability condition limiting the maximal value of the flexocoupling constant f becomes inapplicable, one can expect the instability of the commensurate homogeneous ferroelectric phase (HFP). The instability could lead to the appearance of the incommensurate SMPs in the long-range-ordered phase of ferroelectrics [55]. These results demonstrate the significant influence of the flexocoupling on the scattering spectra in the long-range-ordered phases of different ferroics. However, the thermodynamic analysis of the SPM stability in the ferroics with the square of elastic strain gradient and higher gradients of the order parameters is absent to date.

The gap in the knowledge encouraged us to study the role of flexocoupling between the electric polarization and elastic strain gradients in the stability of SMP in ferroics (such as proper and incipient ferroelectrics) with the square of elastic strain gradient and higher order gradients. Since analytical expressions give insight into the physical nature of the phenomena induced by the flexocoupling and provide the simplest way for quantitative comparison with various experiments, as well as allowing us to determine poorly defined flexoelectric and gradient constants from the comparison with neutron scattering spectra, our primary goal is to derive comprehensive analytical expressions for the conditions of different phases stability and the dispersion law of soft phonons in paraelectric, SMP, and normal ferroelectric phases.

In order to derive the analytical expressions from the LGD free energy, which includes the higher gradient terms, static, and dynamic flexocoupling, we were subjected to restrict our consideration by uniaxial ferroelectrics with one component of the spontaneous polarization and strain. These restrictions can be called the scalar approximation. The consequence of this approximation is the occurrence of only one optical and one acoustic mode in the soft phonon dispersion law, which interact via electrostriction and flexoelectric couplings. The simplified dispersion law cannot describe the interaction between different transverse and longitudinal optical modes and three acoustic modes induced by cooperative effects, flexoelectric, and electrostriction couplings in the ferroelectric phase of multiaxial ferroelectric such as perovskites $BiFeO_3$,$BaTiO_3$, or (Pb,Zr)TiO_3 [55]. Moreover, the coupling between different optical phonon modes can either act cooperatively with the flexocoupling or against it [see, e.g., the models by Kappler and Walker [56] and Hlinka *et al.* [57], adopted for organic ferroelectrics such as $(CH_3)_3NCH_2COO{\cdot}CaCl_2{\cdot}2H_2O$]. If two or more optical modes are considered, their mutual coupling contributes to the SMP appearance similarly to the flexoelectricity standing alone [57].

Taking into account the limitations of the scalar approximation validity, we can reasonably apply obtained analytical results to describe the experimentally observed phonon dispersion in uniaxial ferroics only, e.g., for commensurate ferroelectric $Sn_2P_2S_6$ and incommensurate ferroelectric $Sn_2P_2Se_6$. We choose the monoclinic ferroelectrics $Sn_2P_2(Se_xS_{1-x})_6$ due to their fascinating phase diagrams, relatively well-known material parameters [58–60], and reliable neutron scattering experimental data [61,62]. Rather unexpectedly, we determined that the scalar theory describes semiquantitatively the soft phonon dispersion in the incipient ferroelectric $SrTiO_3$ [43], as well in the paraelectric phase of perovskite ferroelectric $PbTiO_3$ [44],

probably because the interaction between different phonon modes appeared relatively small in the ferroics.

II. SCALAR APPROXIMATION IN THE FREE ENERGY FUNCTIONAL AND LAGRANGE FUNCTION

The LGD free energy F of a ferroic such as proper or incipient ferroelectric acquires the simplest form for the one-component polarization, P, coupled with the strain tensor component, u, which depend only on the coordinate x in the one-dimensional (1D) case [61]. A more general form of the free energy density, which includes tensors and depends on three coordinates, is listed in Appendix. In the simplest one-component 1D case considered hereinafter, the bulk part of the free energy F, which depends on P, u, and their gradients, has the following form:

$$F_V = \int dx \left(\begin{array}{l} \frac{\alpha(T)}{2} P^2 + \frac{\beta}{4} P^4 + \frac{\gamma}{4} P^6 + \frac{g}{2}\left(\frac{\partial P}{\partial x}\right)^2 + \frac{w}{2}\left(\frac{\partial^2 P}{\partial x^2}\right)^2 + \frac{h}{2} P^2 \left(\frac{\partial P}{\partial x}\right)^2 \\ -PE - \frac{1}{2} P E_d - quP^2 + \frac{c}{2} u^2 + \frac{v}{2}\left(\frac{\partial u}{\partial x}\right)^2 - \frac{f}{2}\left(P\frac{\partial u}{\partial x} - u\frac{\partial P}{\partial x}\right) \end{array} \right). \quad (1a)$$

According to Landau theory [63,64], the coefficient α linearly depends on the temperature T for proper ferroelectrics such as $PbTiO_3$, $BaTiO_3$, $Sn_2P_2(Se_xS_{1-x})_6$, and $\alpha(T) = \alpha_T(T - T_C)$. For incipient ferroelectrics such as $SrTiO_3$, α obeys the Barrett-type formula [65], $\alpha(T) = \alpha_T(T_q \coth(T_q/T) - T_C)$. T_C is the real, or virtual, Curie temperature; T_q is a characteristic temperature. All other coefficients in Eq. (1a) are supposed to be temperature independent. Coefficient $\beta > 0$ for the ferroics with the second order phase transition, and $\beta < 0$ for the first order one. Nonlinear stiffness γ should be non-negative ($\gamma \geqslant 0$) for the stability of the functional (1a) for all P values. Parameters g, w, and v determine the magnitude of the gradient energy. For ferroelectrics with HFP, the gradient coefficients $g > 0$ and $w \geqslant 0$, and the coefficients $g < 0$ and $w > 0$ for ferroelectrics with the incommensurate SMP [66]. The nonlinear gradient parameter h is usually small, so its influence will be neglected hereinafter. The polarization interacts with an external electric field E. Also, we assume that the depolarization field E_d is absent. The case corresponds to the transverse variation of polarization components and strains. The electrostriction coefficient q can be positive or negative. The elastic stiffness c and the strain gradient coefficient v should be always positive for the functional stability. Coefficient f is the component of the static flexocoupling tensor, whose sign is not fixed. The first 11 lines of Table I describe all symbols in the LGD free energy (1a) and contain their numerical values for several ferroelectrics. The known numerical values were collected from Refs. [60,61], and [67–69]. The poorly known and previously unknown values of f, v, w, M, and μ were extracted by us from the fitting of the soft phonon spectra measured by Shirane and Yamada [43] and Eijt *et al.* [61,62]. The fitting details are given in Sec. V.

The Lagrange function $L = \int_t dt(F - K)$ consists of the free energy F given by Eq. (1a) and the kinetic energy

$$K = \int dx \left(\frac{\mu}{2}\left(\frac{\partial P}{\partial t}\right)^2 + M\frac{\partial P}{\partial t}\frac{\partial U}{\partial t} + \frac{\rho}{2}\left(\frac{\partial U}{\partial t}\right)^2 \right), \quad (1b)$$

which includes the dynamic flexocoupling [5,6] with the magnitude M, where ρ is the density of a material and μ is a kinetic coefficient. The elastic displacement component U is related with the strain u as $u = \partial U/\partial x$. The last four lines of Table I describe the parameters of the kinetic energy (1b) and contain the numerical values of M, μ, and ρ for several ferroelectrics.

III. THE ANALYTICAL SOLUTIONS OF LINEARIZED EQUATIONS OF STATE

Thermodynamic equations of state are obtained from the variation of the free energy (1a) on the components of the polarization P and strain u, $\delta F/\delta P = 0$ and $\delta F/\delta u = 0$. The explicit form of the equations is

$$\alpha P + \beta P^3 + \gamma P^5 - g\frac{\partial^2 P}{\partial x^2} + w\frac{\partial^4 P}{\partial x^4} - E - f\frac{\partial u}{\partial x} - 2quP = 0, \quad (2a)$$

$$cu - v\frac{\partial^2 u}{\partial x^2} + f\frac{\partial P}{\partial x} - qP^2 = 0. \quad (2b)$$

Let us find the solution of these equations after their linearization in the vicinity of spontaneous values P_S and u_S. The presentation of linearized solution in the form of the Fourier integral is

$$P = P_S + \int dk \exp(ikx)\tilde{P}, \quad u = u_S + \int dk \exp(ikx)\tilde{u}. \quad (3)$$

Homogeneous spontaneous strain and order parameter values are denoted as P_S and u_S, respectively. The perturbation field is $E = \int dk \exp(ikx)\tilde{E}$.

The spontaneous polarization and strain are absent ($P_S = 0$, $u_S = 0$) in the high temperature parent phase, wherein the coefficient $\alpha > 0$. In the low temperature ordered phase (wherein $\alpha < 0$ and $P_S \neq 0$, $u_S \neq 0$), the spontaneous strain and polarization values can be determined from the equations of state (2) at zero gradients, namely

$$u_S = \frac{q}{c}P_S^2, \quad P_S^2 = \frac{1}{2\gamma}\left(\sqrt{\beta^{*2} - 4\alpha\gamma} - \beta^*\right), \quad (4)$$

where the coefficient $\beta^* = (\beta - 2\frac{q^2}{c})$. Expression (4) is valid for ferroelectrics with the first and second order phase transitions from the ordered phase to the parent phase. In the particular case of the second order phase transition for parameters $\beta^* > 0, \gamma = 0$, the spontaneous polarization value is $P_S^2 = -\alpha/\beta^*$, so the condition $c\beta > 2q^2$ should be valid for the transition realization.

TABLE I. Description of the symbols in the LGD free energy (1a) and kinetic energy (1b) and their numerical values for several ferroelectrics with $g > 0$ and $g < 0$.

Description	Symbol and dimension	Incipient and proper ferroelectrics			
		$SrTiO_3$	$PbTiO_3$	$Sn_2P_2S_6$	$Sn_2P_2Se_6$
Coefficient at P^2	$\alpha(T)$ ($\times C^{-2}\cdot$ mJ)	$\alpha_T\left(T_q \coth\left(\frac{T_q}{T}\right) - T_C\right)$	$\alpha_T(T - T_C)$	$\alpha_T(T - T_C)$	$\alpha_T(T - T_C)$
Inverse Curie-Weiss constant	α_T ($\times 10^5 C^{-2}\cdot$ mJ/K)	15	7.53	16	26
Curie temperature	T_C (K)	$T_C = 30$ $T_q = 54$	752	337	193
LGD coefficient at P^4	β ($\times 10^8$ JC$^{-4}\cdot$ m^5)	81	−2.90	+7.42	−4.8
LGD coefficient at P^6	γ ($\times 10^9$ JC$^{-6}\cdot$ m^9)	0 (data absent)	1.56	35	85
Electrostriction coefficient	q($\times 10^9$ Jm/C^2)	2.4 since $q_{44} = 2.4$	3 since $q_{44} = 3.0$	4 (reference interval 1.6– 4.7)	5 (defined from acoustic mode tilt)
Elastic stiffness coefficient	c ($\times 10^{10}$ Pa)	12.7 since $c_{44} = 12.7$	9 since $c_{44} = 9.0$	1.6 since $c_{44} = 1.6 \pm 0.3$	1.6 (defined from acoustic mode tilt)
Gradient coefficient at $(\nabla P)^2$	g ($\times 10^{-10}$ C^{-2}m^{3}J)	2 (fitting par.)	0.5 since$g_{44} = 0.5$	0.5 (fitting parameter)	−0.6 (fitting parameter)
Gradient coefficient at $(\nabla^2 P)^4$	w ($\times 10^{-29}$ Jm^5/C^2)	0 (data absent)	0 (data absent)	1.8 (reference value 1.8)	2.5 (reference value 2.2)
Elastic strain gradient $(\nabla u)^2$	v ($\times 10^{-9}$ V s^2/m^2)	12 (fitting parameter)	8 (fitting parameter)	5 (fitting parameter)	1 (fitting parameter)
Static flexo-coefficient	f(V)	±1.5 (fitting parameter)	± 2.0 (fitting parameter)	$f_{44} = \pm(1.6–1.8)$ (fitting parameter)	±1.0 (fitting parameter)
Dynamic flexo-coefficient	M ($\times 10^{-8}$ Vs^2/m^2)	± 24 (fitting parameter)	± 2.0 (fitting parameter)	± 2.5 (fitting parameter)	±1.5 (fitting parameter)
Kinetic coefficient	μ ($\times 10^{-18}$ s^2 mJ)	22 (fitting parameter)	1.59 (fitting parameter)	11.0 (fitting parameter)	14.5 (fitting parameter)
Material density at normal conditions	ρ ($\times 10^3$ kg/m^3)	4.930 at 120 K	8.086 (at T > Tc)	1.801	2.547
Lattice constant	a (nm)	$a_x = a_y = a_z$ = 0.395 at 120 K	$a_x = a_y = a_z$ = 0.397 at (760–800) K	$a_x \approx 0.93$, $a_y \approx 0.75$, $a_z \approx$ 0.65 at (200–350) K	$a_x \approx 0.97$, $a_y \approx 0.77$, $a_z \approx$ 0.68 at (200–350) K

After linearization, Eqs. (2a) and (2b) acquire the form,

$$\left(\alpha + 3\beta P_S^2 + 5\gamma P_S^4 - 2qu_S + gk^2 + wk^4\right)\tilde{P} - (ifk + 2qP_S)\tilde{u} = \tilde{E}, \tag{5a}$$

$$(c + vk^2)\tilde{u} + (ifk - 2qP_S)\tilde{P} = 0. \tag{5b}$$

The linearized solution of Eqs. (5a) and (5b) is

$$\tilde{u} = -\frac{(ifk - 2qP_S)}{(c + vk^2)}\tilde{\chi}(k)\tilde{E}, \quad \tilde{P} = \tilde{\chi}(k)\tilde{E}. \tag{6}$$

The linear susceptibility $\tilde{\chi}(k)$ introduced in Eq. (6) is given by the expression

$$\tilde{\chi}(k) = \left(\alpha + 3\beta P_S^2 + 5\gamma P_S^4 - 2qu_S + gk^2 + wk^4 - \frac{4q^2P_S^2 + f^2k^2}{c + vk^2}\right)^{-1}. \tag{7}$$

The condition of the solution (6) instability corresponds to the divergence of the susceptibility (7). After substituting expression (4) for u_S into Eq. (7), the instability condition acquires the form

$$\alpha_S + g^{\text{eff}}k^2 + \left(\frac{gv}{c} + w\right)k^4 + \frac{wv}{c}k^6 - 4\frac{q^2}{c}P_S^2 = 0. \tag{8}$$

Here, parameter α_S and effective gradient coefficient g^{eff} are introduced:

$$\alpha_S = \alpha + \left(3\beta - 2\frac{q^2}{c}\right)P_S^2 + 5\gamma P_S^4, \tag{9a}$$

$$g^{\text{eff}} = \left(g + \frac{\alpha_S v}{c} - \frac{f^2}{c}\right). \tag{9b}$$

One can show that parameter α_S is always positive. It is equal to α in the parent phase, wherein $P_S = 0$. The inhomogeneous SMP can appear if the renormalized gradient coefficient (9b) becomes negative. Since the elastic stiffness is always positive ($c > 0$), the homogeneous phase $P = P_S$ is absolutely stable under the condition $f^2 < cg + \alpha_S v$. The condition is temperature dependent because of the temperature dependence of the coefficient $\alpha_S(T)$.

If the strain gradient coefficient v is zero, the condition $f^2 < cg + \alpha_S v$ reduces to the inequality $f^2 < cg$, which is nothing more that the scalar form of the tensor relation $f_{klmn}^2 < g_{ijkl}c_{ijmn}$ from Ref. [16]. Later on, the condition

TABLE II. Description of dimensionless parameters and their numerical values for several ferroelectrics.

Dimensionless parameter	Analytical expression	Numerical value for incipient and proper ferroelectrics			
		$SrTiO_3$ above 100 K	$PbTiO_3$ at (730–800) K	$Sn_2P_2S_6$* at (200–440) K	$Sn_2P_2Se_6$ at (100–223) K
Wave vector	$k^* = ak/\pi$	variable	variable	variable	variable
Lattice constant	$a^* = \sqrt{c/2v}\,(a/\pi)$	0.07	0.30	0.26 (a_z*at 200 K) 0.3 (a_y*at 440 K)	0.61
Static flexoconstant	$F^* = f^2/(cg)$	0.09	0.89	3.20 (f_{44}*at 200 K) 4.05 (f_{55}*at 440 K)	−1.04
Reduced temperature	$\alpha_v^* = \alpha_S(T)v/(cg)$	0.64 (at 120 K)	0.04 (at 783 K)	1.03 (at440 K) 3.97 (at 200 K)	−0.08 (at 223 K) −0.88 (at 100 K)
Stiffness constant	$\alpha_T^* = v\alpha_T T_C/(gc)$	0.21	1.01	3.37	−4.18
High gradient coefficient	$w^* = cw/(vg)$	0	0	1.15	−6.67
Electrostriction parameter	$Q^* = 4q^2P_S^2/(c\alpha_S)$	0	0 (at 783 K) 0.63 (at 733 K)	0 (at 440 K) 0.44 (at 200 K)	0 (at 223 K) 0.42 (at 100 K)
Electrostriction ratio	$2q^2/\beta c$	0.011	−0.689	2.695	−6.510
Dynamic flexoconstant	$M^* = cM/(2\rho f)$	2.06	0.056	0.062 (at 440 K) 0.069 (at 440 K)	0.047
Kinetic coefficient	$\mu^* = c\mu/(2g\rho)$	1.41	0.18	0.89	−0.76
Phonon frequency	$\omega^* = \sqrt{4v\rho}\omega/c$	variable	variable	variable	Variable
Characteristic frequency	$\omega_0 = c/\sqrt{4v\rho}$	$8.3 \times 10^{12}\ s^{-1}$	$5.6 \times 10^{12}\ s^{-1}$	$2.7 \times 10^{12}\ s^{-1}$	$5.0 \times 10^{12}\ s^{-1}$

*$S_2P_2S_6$ fitting parameters have been determined for $k \uparrow\uparrow z$ at 440 K and for $k \uparrow\uparrow y$ at 200 K. Because of this, the lattice constants and flexoelectric coefficients can be different for different directions.

$f_{44}^2 < g_{44}c_{44}$ (along with other similar conditions) has been derived for perovskite symmetry by Yudin, Ahluwalia, and Tagantsev [37] and interpreted as the upper limit for the magnitude of the static flexoelectric tensor without the gradient term $\frac{v_{ijklmn}}{2}(\frac{\partial u_{ij}}{\partial x_m}\frac{\partial u_{kl}}{\partial x_n})$ and other higher order gradients in the free energy of ferroelectrics. However, Mao and Purohit derived more complex stability conditions for the spatially confined systems with nonzero strain gradient tensor $v_{ijklmn} \neq 0$ [see Eq. (28) in Ref. [40]], which can be reduced to the simple inequality $f^2 < \alpha v$ in the scalar approximation because the authors assume that $g = 0$ in the designations of this paper. Following Ref. [37], Stengel used the inequality $f^2 < cg$ for the critical value of the flexoelectric coefficient [see Eq. (106) in Ref. [41]].

Below, we will show that the necessary temperature dependent condition $g^{\text{eff}} < 0$ per se is not sufficient for the stability of the spatial modulation onset.

If one can neglect the smallest term vwk^6 in Eq. (8), it reduces to the biquadratic equation with four roots:

$$k_{1,2}^{\pm} = \pm\sqrt{\frac{cg}{2(gv+cw)}\left(\frac{f^2}{cg} - 1 - \frac{\alpha_S v}{cg} \pm \sqrt{\left(\frac{f^2}{cg} - 1 - \frac{\alpha_S v}{cg}\right)^2 - 4\frac{(gv+cw)}{cg^2}\left(\alpha_S - 4\frac{q^2}{c}\eta_S^2\right)}\right)}. \tag{10}$$

Subscripts 1 and 2 in expression (10) correspond to the + and − signs before the outer square root. The solution $k_{1,2}^{+}$ corresponds to the + sign before the inner square root, and root $k_{1,2}^{-}$ corresponds to the − sign before it.

Let us introduce the dimensionless wave vector k^* and parameters a^*, F^*, α_v^*, w^*, Q^*:

$$k^* = \frac{ak}{\pi}, \quad a^* = \frac{a}{\pi}\sqrt{\frac{c}{2v}}, \quad F^* = \frac{f^2}{cg}, \quad \alpha_v^* = \frac{\alpha_S v}{cg}, \quad w^* = \frac{cw}{vg}, \quad Q^* = 4\frac{q^2\eta_S^2}{c\alpha_S}, \tag{11}$$

where a is the lattice constant. Note that the case $g = 0$ is excluded from the analysis for chosen dimensionless variables (11), since we consider ferroelectrics with composition far from the Lifshitz point.

Description of these dimensionless parameters and their numerical values for several ferroelectrics are given in the first eight lines of Table II. The next four lines describe the dimensionless parameters of the kinetic energy (1b), which will be introduced in Sec. IV.

Using the dimensionless parameters (11), we can represent the positive solutions (10) in the following form:

$$k_{\pm}^* = a^*\sqrt{\frac{1}{w^*+1}(F^* - 1 - \alpha_v^* \pm \sqrt{(F^* - 1 - \alpha_v^*)^2 - 4\alpha_v^*(w^*+1)(1-Q^*)})}. \tag{12}$$

The wave vector k_+^* corresponds to the + sign before the inner square root in Eq. (12), and k_-^* corresponds to the − sign before it.

Note that the parameter α_v^* is proportional to the product of the temperature dependent coefficient α_S and the strain gradient coefficient v. For the ferroelectrics with the second order phase transitions with parameters $\beta^* > 0$ and $\gamma = 0$, the square of the order parameter is $P_S^2 = -\alpha/\beta^* \cong \alpha_T(T_C - T)/(\beta - 2q^2/c)$. From the expression, one determines that the coefficient α_v^* linearly depends on T in the high temperature parent phase and low temperature ordered phase:

$$\alpha_v^*(T) = \begin{cases} \alpha_T^*\left(\frac{T}{T_C} - 1\right), & \frac{T}{T_C} > 1, \\ \frac{2\alpha_T^*}{(1-(2q^2/\beta c))}\left(1 - \frac{T}{T_C}\right), & 0 < \frac{T}{T_C} < 1. \end{cases} \quad (13)$$

The dimensionless parameter $\alpha_T^* = \frac{v\alpha_T T_C}{gc}$ is introduced in Eq. (13). The parameter is positive for $g > 0$ and negative for $g < 0$.

Note that it makes sense to study the phase diagram in dependence on the reduced temperature $\alpha_v^* \sim \alpha_T^*(1 - T/T_C)$ and flexoconstant $F^* \sim f^2/g$. Both parameters, α_v^* and F^*, are proportional to $1/g$, positive for $g > 0$, and negative for $g < 0$.

Expression (9b) for g^{eff} written in dimensionless variables (11) acquires the form $\frac{g^{\text{eff}}}{g} = (1 + \frac{\alpha_S v}{gc} - \frac{f^2}{gc}) \equiv 1 + \alpha_v^* - F^*$. Thus, the necessary condition of the SMP appearance $g^{\text{eff}} < 0$, written in dimensionless variables (11), is equivalent to the inequality $\text{sign}(g)(1 + \alpha_v^* - F^*) < 0$. However, as one can see from Eq. (12), the condition $g^{\text{eff}} < 0$ is not sufficient per se because the additional condition of positive inner determinant, $(F^* - 1 - \alpha_v^*)^2 \geqslant 4\alpha_v^*(w^* + 1)(1 - Q^*)$, should be valid.

IV. THE IMPACT OF ELASTIC STRAIN GRADIENT AND FLEXOCOUPLING ON THE STABILITY OF SPATIALLY MODULATED PHASES

Let us analyze expression (12) for different signs of g. Since $g > 0$ for proper and incipient ferroelectrics without the incommensurate phase at $f = 0$, the parameters $F^* \geqslant 0$, $\alpha_v^* \geqslant 0$, $Q^* \geqslant 0$, and $w^* \geqslant 0$ for the case. Hereinafter, we put $w^* = 0$ for ferroelectrics with $g > 0$ for the sake of simplicity. The parameters $F^* \leqslant 0$, $\alpha_v^* \leqslant 0$, $Q^* \geqslant 0$, and $w^* < 0$ for ferroelectrics with $g < 0$.

The typical values of dimensionless parameters (11) can be estimated from Table II. In particular, dimensionless parameters can change in the ranges $0 \leqslant Q^* < 1, 0 \leqslant w^* < 1$ for $g > 0$, and $w^* < -2$ for $g < 0$; $-5 < F^* < 5, -5 < \alpha_v{}^* < 5$, and $0.1 < a^* < 1$ for both signs of g, and $-0.5 < k^* < 0.5$ in the first Brillouin zone.

A. Ferroelectrics with positive coefficient of polarization gradient

Inequalities $4\alpha_v^*(w^* + 1)(1 - Q^*) > 0$, $F^* \geqslant 0$, $\alpha_v^* \geqslant 0$, $0 \leqslant Q^* < 1$, and $w^* \geqslant 0$ are valid for $g > 0$. Using all of these inequalities in Eq. (12), we derived that the HFP is thermodynamically stable under the condition $(F^* - 1 - \alpha_v^*)^2 < 4\alpha_v^*(w^* + 1)(1 - Q^*)$, and the SMP with modulation periods $k_\pm^*$ can appear under conditions $(F^* - 1 - \alpha_v^*)^2 \geqslant 4\alpha_v^*(w^* + 1)(1 - Q^*)$ and $F^* \geqslant 1 + \alpha_v^*$. Therefore, the necessary condition of SMP appearance is the fulfillment of inequality $(1 + \alpha_v^* - F^*) < 0$. All these inequalities give us the necessary and sufficient conditions of the HFP and SMP stability in ferroelectrics with $g > 0$:

$$0 \leqslant F^* < 1 + \alpha_v^* + 2\sqrt{\alpha_v^*(w^* + 1)(1 - Q^*)} \quad \text{(HFP phase is stable)}, \quad (14a)$$

$$F^* \geqslant 1 + \alpha_v^* + 2\sqrt{\alpha_v^*(w^* + 1)(1 - Q^*)} \quad \text{(SMP phase is stable)}. \quad (14b)$$

The phase diagram of the ferroelectrics with $g > 0$ is shown in the left-hand side of Fig. 1(a), where $\alpha_v^* \geqslant 0$ and $F^* \geqslant 0$. As one can see from the figure, the minimal positive value of the flexoconstant F_{cr}^* required for SMP appearance is $F_{cr}^* = 1$; the case corresponds to $\alpha_v^* = 0$. In this way, HFP is absolutely stable for $F^* < 1$ at $\alpha_v^* = 0$. The value of F_{cr}^* monotonically increases with α_v^* increasing, in accordance with the formula $F_{cr}^*(\alpha_v^*) = 1 + \alpha_v^* + 2\sqrt{\alpha_v^*(w^* + 1)(1 - Q^*)}$ [see red curves in the left-hand side of Fig. 1(a)].

The dependence of the critical value of dimensionless flexoconstant F_{cr}^* on relative temperature T/T_C and the temperature dependence of the critical value of flexoelectric coefficient

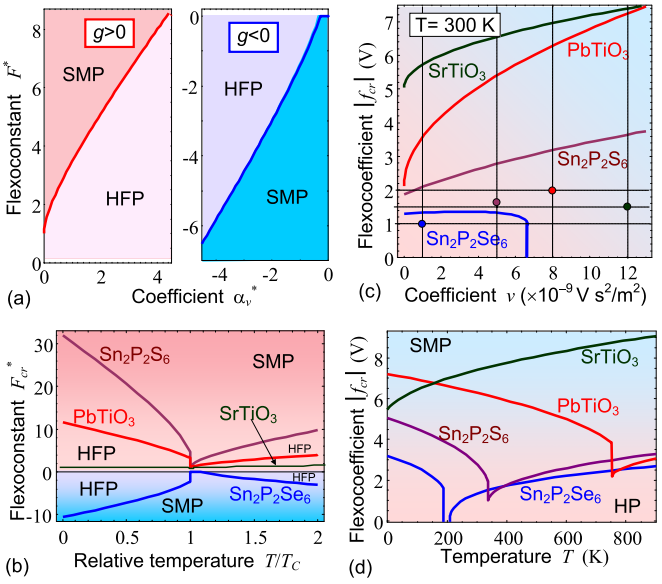

FIG. 1. (a) Diagrams of the spatially modulated phase (SMP) and homogeneous ferroelectric phase (HFP) stability in ferroics with $g > 0$ (right side) and $g < 0$ (left side) plotted in dimensionless coordinates—flexoconstant F^* and reduced temperature α_v^*. Parameters $Q^* = 0.5$, $F^* \leqslant 0, a_v{}^* \leqslant 0$, and $w^* = -2$ for the case $g < 0$; $F^* \geqslant 0, \alpha_v{}^* \geqslant 0$, and $w^* = 0$ for $g > 0$. (b) Temperature dependence of the flexoconstant critical value F_{cr}^*. (c), (d) Dependence of the flexoelectric coefficient critical value f_{cr}^* on the strain gradient constant v (c) and temperature T (d). The curves in (b)–(d) are calculated for dimension and dimensionless parameters of incipient ferroelectric $SrTiO_3$ and proper ferroelectrics $PbTiO_3$, $Sn_2P_2S_6$, and $Sn_2P_2Se_6$ from Tables I and II, with the exception of f values, which change in (b) and (d), and v values, which change in (c). Points in (c) correspond to the values of f and v, determined from the phonon spectra of ferroelectrics shown in Fig. 4.

$f_{cr}(T)$ are nonmonotonic with a pronounced peculiarity (jumps look like "gull wings") at the Curie temperature for proper ferroelectrics [see the curves for $PbTiO_3$ and $Sn_2P_2S_6$ in Figs. 1(b) and 1(d)]. The peculiarity originates from the break in the parameter $\alpha_v^*(T)$ at the Curie temperature T_C [see, e.g., Eq. (13)]. The peculiarity is absent for incipient ferroelectrics since $\alpha_v^*(T)$ monotonically decreases as T increases, in accordance with the Barrett-type formula for these materials. Therefore, the critical values F_{cr}^* and $|f_{cr}|$ slightly increase with temperature increase for incipient ferroelectrics with $g > 0$ [see the curves for $SrTiO_3$ in Figs. 1(b) and 1(d)]. The critical value of the flexoelectric coefficient $|f_{cr}|$ monotonically increases, with the coefficient v increasing for $g > 0$ [see the curves for $SrTiO_3$,$PbTiO_3$, and $Sn_2P_2S_6$ in Fig. 1(c)].

Note that the curves in Figs. 1(b)–1(d) are calculated for the parameters of ferroelectrics $SrTiO_3$,$PbTiO_3$, and $Sn_2P_2S_6$ from Tables I and II, except for the f values, which are variables in Figs. 1(b) and 1(d), and v values, which vary in Fig. 1(c). Dark green, red, and maroon colored points in Fig. 1(c) correspond to the values of f and v determined from the phonon spectra of $SrTiO_3$,$PbTiO_3$, and $Sn_2P_2S_6$ considered in Sec. VI. The points are located significantly lower than the curves $|f_{cr}(v)|$ for these materials, indicating that the SMP appearance is impossible at 300 K for realistic values of the parameters f and v, as anticipated from experiment because $SrTiO_3$ is paraelectric and $PbTiO_3$ and $Sn_2P_2S_6$ are commensurate ferroelectrics at room temperature. The critical values F_{cr}^* and f_{cr} are essentially higher for $SrTiO_3$ and $PbTiO_3$ in comparison with the values for $Sn_2P_2S_6$.

The dependences of the wave vectors k_+^* and k_-^* on the dimensionless flexoconstant F^* and reduced temperature α_v^* are shown in the right-hand side of Figs. 2(a) and 2(b), respectively. The gap of width d corresponding to the α_v^* range, for which both wave vectors k_+^* and k_-^* are absent, exists for all curves calculated for different values of α_v^* and $F^* < F_{cr}^*$ [see the left-hand side of Fig. 2(a)]. The gap width d is conditioned by the value $F_{cr}^*(\alpha_v^*)$, and it increases as α_v^* increases. Equal wave vectors appear under the condition $F^* = F_{cr}^*$, namely $k_-^*(\alpha_v^*, F_{cr}^*) = k_+^*(\alpha_v^*, F_{cr}^*)$. At $F^* > F_{cr}^*$, the wave vector k_-^* decreases, and k_+^* increases with F^* increasing [see dashed and solid curves in the left-hand side of Fig. 2(a)]. There is the maximal positive value $\alpha_{cr}^*(F^*)$ required for the SMP appearance at fixed F^* value. Wave vectors are equal under the condition $\alpha_v^* = \alpha_{cr}^*$, namely $k_-^*(\alpha_{cr}^*, F^*) = k_+^*(\alpha_{cr}^*, F^*)$. Under the condition $\alpha_v^* < \alpha_{cr}^*$, the wave vector k_-^* increases, and k_+^* decreases as the parameter α_v^* increases [compare dashed and solid curves in the right-hand side of Fig. 2(b)].

B. Ferroelectrics with negative coefficient of polarization gradient

The stability conditions of the HFP and SMP are more complex for negative g because they are different for the cases $-1 < w^* \leqslant 0$ and $w^* < -1$. In accordance with our estimates, the most realistic and interesting situation corresponds to the case $w^* < -1$, for which we continue our analysis. For the case $w^* < -1$, the inequality $4\alpha_v^*(w^*+1)(1-Q^*) > 0$ is valid. Also, the inequalities $F^* \leqslant 0$, $\alpha_v^* < 0$, and $0 \leqslant Q^* < 1$ are valid for the case $g < 0$. Using all these inequalities in

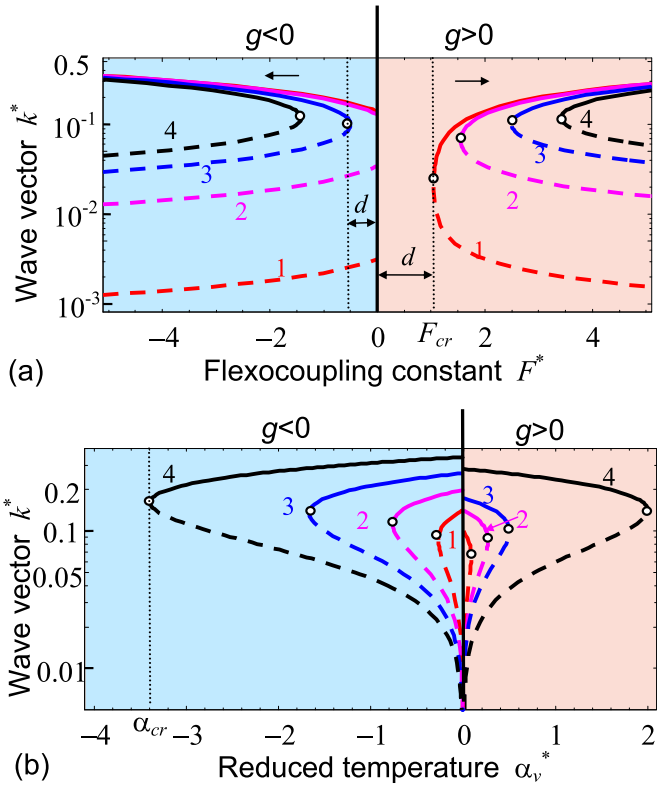

FIG. 2. Dependences of the wave vectors k_+^* (solid curves) and k_-^* (dashed curves) on the flexoconstant F^* (a) and reduced temperature α_v^* (b). Different curves are calculated for several values of $\alpha_v^* = 0.001, 0.1, 0.5, 1$ for $g > 0$ and $\alpha_v^* = -0.001, -0.1, -0.5, -1$ for $g < 0$ [curves 1–4 in plot (a)]; $F^* = 1.5, 2, 2.5, 5$ for $g > 0$; and $F^* = -0.001, -1, -2.5, -5$ for $g < 0$ [curves 1–4 in plot (b)]. Parameters $Q^* = 0.5$, $a^* = 0.1$, and $w^* = -2$ for ferroelectrics with $g > 0$, and $w^* = 0$ for $g < 0$.

Eq. (12), we derived that the HFP is thermodynamically stable under the condition $(F^* - 1 - \alpha_v^*)^2 < 4\alpha_v^*(w^*+1)(1-Q^*)$ (the same as for $g > 0$), and the SMP with modulation periods given by Eq. (12) can appear under the conditions $F^* \leqslant 0$, $F^* \leqslant 1 + \alpha_v^*$, and $(F^* - 1 - \alpha_v^*)^2 \geqslant 4\alpha_v^*(w^*+1)(1-Q^*)$. The necessary condition of the SMP appearance is the inequality $(1 + \alpha_v^* - F^*) < 0$. All these inequalities lead to the necessary and sufficient conditions of the HFP and SMP stability in ferroelectrics with $g < 0$:

$$1 + \alpha_v^* - 2\sqrt{\alpha_v^*(w^*+1)(1-Q^*)} < F^* < 0, \quad \text{(HFP phase is stable)}, \tag{15a}$$

$$F^* \leqslant 0 \text{ and } F^* \leqslant 1 + \alpha_v^* - 2\sqrt{\alpha_v^*(w^*+1)(1-Q^*)} \quad \text{(SMP phase is stable)} \tag{15b}$$

The phase diagram of the ferroelectrics with $g < 0$ is shown in the right-hand side of Fig. 1(a), where $\alpha_v^* \leqslant 0$ and $F^* \leqslant 0$. In contrast to ferroelectrics with $g > 0$, the SMP appears at $F^* = 0$, and $\alpha_v^* \geqslant -0.3$ for $g < 0$. The negative critical value of the flexoconstant $F_{cr}^*(\alpha_v^*)$ occurs if $\alpha_v^* < -0.3$, and its absolute value increases quasilinearly with $|\alpha_v^*|$ increasing, in accordance with the formula $F_{cr}^*(\alpha_v^*) = 1 + \alpha_v^* - 2\sqrt{\alpha_v^*(w^*+1)(1-Q^*)}$ [see blue curves in the right-hand side of Fig. 1(a)].

Similar to the case of ferroelectrics with $g > 0$, for ferroelectrics with $g < 0$ the temperature dependences of the critical values F^*_{cr} and $f_{cr}(T)$ are nonmonotonic with a pronounced peculiarity at the Curie temperature [see the curves for $Sn_2P_2Se_6$ in Figs. 1(b) and 1(d)]. The critical value of the flexocoefficient $|f_{cr}|$ monotonically increases with increase of the strain gradient coefficient v [see the curve for $Sn_2P_2Se_6$ in Fig. 1(c)].

Note that the curves in Figs. 1(b)–1(d) are calculated for parameters of $Sn_2P_2Se_6$ from Tables I and II, except for the f values, which are variables in Figs. 1(b) and 1(d), and v values, which vary in Fig. 1(c). The blue point in Fig. 1(c) corresponds to the values of f and v, determined from the phonon spectra of $Sn_2P_2Se_6$ shown in Figs. 4(c)–4(d). The point is located a bit lower than the curve $|f_{cr}(v)|$ for $Sn_2P_2Se_6$ that indicates the SMP instability at room temperature as anticipated from experiments because $Sn_2P_2S_6$ is a paraelectric at the temperature. $Sn_2P_2Se_6$ has the region of the SMP (even at $f = 0$) for temperatures slightly higher that the Curie temperature 193 K.

The dependences of the wave vectors k^*_+ and k^*_- on the flexoconstant F^* and coefficient α^*_v are shown in the left-hand side of Figs. 2(a) and 2(b), respectively. The gap of thickness d exists only for the two curves, corresponding to the highest values of $|\alpha^*_v|$, as it follows from the dependence $F^*_{cr}(\alpha^*_v)$ [see the right-hand side of Fig. 2(a)]. Wave vectors are equal for the case $F^* = F^*_{cr}$, namely $k^*_-(\alpha^*_v, F^*_{cr}) = k^*_+(\alpha^*_v, F^*_{cr})$. For the case $F^* < F^*_{cr}$, the wave vector k^*_- decreases as $|F^*|$ increases, while k^*_+ increases as $|F^*|$ increases [compare dashed and solid curves in the right-hand side of Fig. 2(a)]. There is the minimal negative value $\alpha^*_{cr}(F^*)$ of the SMP appearance at fixed F^* value. Wave vectors are equal under the condition $\alpha^*_v = \alpha^*_{cr}$, for which $k^*_-(\alpha^*_v, F^*) = k^*_+(\alpha^*_v, F^*)$. At $|\alpha^*_v| < |\alpha^*_{cr}|$, wave vector k^*_- increases, and k^*_+ decreases as $|\alpha^*_v|$ increases [compare dashed and solid curves in the right-hand side of Fig. 2(b)].

To resume the results of the section, performed analysis showed that the fundamental upper limits for the maximal values of the static flexoelectric coefficients [37], which exist under the absence of the higher order gradient terms in the free energy (1b), should be substituted by the temperature dependent conditions (14) or (15) corresponding to the HFP stability or SPM phase appearance.

V. SOFT PHONON DISPERSION IN THE SCALAR APPROXIMATION

Soft phonon dispersion can be calculated from the time-dependent dynamic equations of state for the polarization and elastic displacement components P and U, respectively [55]. The dynamic equations of state are obtained from the variation of the Lagrange function $L = \int_t dt(F - K)$ on P and U, where the free energy F is given by Eq. (1a), and the kinetic energy K is given by Eq. (1b). The explicit form of the equations $\delta L/\delta U = 0$ and $\delta L/\delta P = 0$ is

$$v\frac{\partial^4 U}{\partial x^4} + \rho\frac{\partial^2 U}{\partial t^2} - c\frac{\partial^2 U}{\partial x^2} - f\frac{\partial^2 P}{\partial x^2} + 2qP\frac{\partial P}{\partial x} + M\frac{\partial^2 P}{\partial t^2} = 0, \tag{16a}$$

$$\Gamma\frac{\partial P}{\partial t} + \mu\frac{\partial^2 P}{\partial t^2} + \alpha P + \beta P^3 + \gamma P^5 - g\frac{\partial^2 P}{\partial x^2} + w\frac{\partial^4 P}{\partial x^4} - f\frac{\partial^2 U}{\partial x^2} - 2qP\frac{\partial U}{\partial x} + M\frac{\partial^2 U}{\partial t^2} = E. \tag{16b}$$

Note that the Khalatnikov mechanism of polarization relaxation, namely the term $\Gamma\partial P/\partial t$, is included in Eq. (16b); Γ is a kinetic coefficient.

The solution of dynamic Eq. (16) was found after the linearization in the vicinity of spontaneous values P_S and u_S, respectively. Using Fourier integrals for polarization, $P = P_S + \int dk \exp(ikx + i\omega t)\tilde{P}$, displacement $U = u_S x + \int dk \exp(ikx + i\omega t)\tilde{U}$, and perturbation field, $E = \int dk \exp(ikx + i\omega t)\tilde{E}$, the linearized Eq. (16) acquires the form

$$(vk^4 + ck^2 - \rho\omega^2)\tilde{U} + (fk^2 + 2ikqP_S - M\omega^2)\tilde{P} = 0, \tag{17a}$$

$$\left(i\omega\Gamma - \mu\omega^2 + \alpha + 3\beta P_S^2 + 5\gamma P_S^4 - 2qu_S + gk^2 + wk^4\right)\tilde{P} + (fk^2 - 2iqkP_S - M\omega^2)\tilde{U} = \tilde{E}. \tag{17b}$$

The solution of Eq. (17) in the spatial (k) and frequency (ω) domains was found after elementary transformations:

$$\tilde{U} = -\frac{fk^2 + 2ikqP_S - M\omega^2}{vk^4 + ck^2 - \rho\omega^2}\tilde{P}, \tag{18a}$$

$$\tilde{P} = \tilde{\chi}(k,\omega)\tilde{E}. \tag{18b}$$

The generalized linear susceptibility $\tilde{\chi}(k,\omega)$ introduced in Eq. (18b) is given by expression

$$\tilde{\chi}(k,\omega) = \left(i\omega\Gamma - \mu\omega^2 + \alpha + 3\beta P_S^2 + 5\gamma P_S^4 - 2qu_S + gk^2 + wk^4 - \frac{\left(fk^2 - M\omega^2\right)^2 + 4k^2q^2P_S^2}{vk^4 + ck^2 - \rho\omega^2}\right)^{-1}. \tag{19}$$

The condition of the susceptibility (19) divergence leads to the equation for phonon dispersion $\omega(k)$:

$$i\omega\Gamma - \mu\omega^2 + \alpha + 3\beta P_S^2 + 5\gamma P_S^4 - 2qu_S + gk^2 + wk^4 - \frac{(fk^2 - M\omega^2)^2 + 4k^2q^2P_S^2}{vk^4 + ck^2 - \rho\omega^2} = 0. \tag{20}$$

Using the solution $u_S = qP_S^2/c$ [Eq. (4)] and the definition of $\alpha_S = \alpha + (3\beta - 2(q^2/c))P_S^2 + 5\gamma P_S^4$ [Eq. (9a)] and neglecting the damping ($\Gamma \rightarrow 0$), one can rewrite Eqs. (19) and (20) in the form,

$$\tilde{\chi}(k,\omega) = \left(-\mu\omega^2 + \alpha_S + gk^2 + wk^4 - \frac{(fk^2 - M\omega^2)^2 + 4k^2q^2P_S^2}{vk^4 + ck^2 - \rho\omega^2}\right)^{-1}, \tag{21}$$

$$(-\mu\omega^2 + \alpha_S + gk^2 + wk^4)(vk^4 + ck^2 - \rho\omega^2) - (fk^2 - M\omega^2)^2 - 4k^2q^2P_S^2 = 0. \tag{22}$$

The solution of biquadratic Eq. (22) can be represented in the form,

$$\omega^2 = \frac{C \pm \sqrt{D}}{2(\mu\rho - M^2)}, \tag{23a}$$

wherein the constant C and determinant D are introduced

$$C = \alpha_S\rho + (c\mu - 2fM + g\rho)k^2 + (\mu v + \rho w)k^4, \tag{23b}$$

$$D = C^2 - 4(\mu\rho - M^2)k^2(\alpha_S c - 4q^2P_S^2 + (cg + \alpha_S v - f^2)k^2 + (gv + cw)k^4 + vwk^6). \tag{23c}$$

Let us introduce the dimensionless frequency ω^* and parameters M^* and μ^* in the following way:

$$\omega^* = \frac{\sqrt{4v\rho}}{c}\omega, \quad M^* = \frac{cM}{2\rho f}, \quad \mu^* = \frac{c\mu}{2g\rho}. \tag{24}$$

Description of these dimensionless parameters and their numerical values for several ferroelectrics are given in the last four lines of Table II.

Using the definitions of dimensionless wave vector k^* and frequency ω^* and parameters (11) and (24), one can rewrite Eq. (22) in the dimensionless variables,

$$\left(-\mu^*\omega^{*2} + 2\alpha_v^* + k^{*2} + \frac{w^*}{2}k^{*4}\right)(k^{*4} + 2k^{*2} - \omega^{*2}) - 2F^*(k^{*2} - M^*\omega^{*2})^2 - 4\alpha_v^*Q^*k^{*2} = 0. \tag{25}$$

The solution of Eq. (23) acquires the form,

$$\omega^{*2} = \frac{(C^* \pm \sqrt{D^*})}{2(\mu^* - 2F^*M^{*2})}, \tag{26a}$$

$$C^* = 2\alpha_v^* + (k^*/a^*)^2(2\mu^* + 1 - 4F^*M^*) + (k^*/a^*)^4(\mu^* + w^*), \tag{26b}$$

$$D^* = C^{*2} + 4(k^*/a^*)^2(2F^*M^{*2} - \mu^*)\begin{pmatrix}4\alpha_v^*(1 - Q^*) + 2(k^*/a^*)^2(1 - F^* + \alpha_v^*)\\ +w^*(k^*/a^*)^6 + (k^*/a^*)^4(1 + 2w^*)\end{pmatrix}. \tag{26c}$$

Dispersion relation (26a) contains one optical (O) and one acoustic (A) phonon modes. The O mode is in fact transverse, and the A mode can be longitudinal or transverse. The gap between these modes is proportional to the value $\frac{\sqrt{D^*}}{2F^*M^{*2}-\mu^*}$, which gives us the possibility to determine the magnitude of the flexocoupling constants from the analytical expressions (26).

The dependences of the dimensionless phonon frequency ω^* on the wave vector k^* are shown in Figs. 3(a) and 3(b) for ferroelectrics with $g > 0$ and in Figs. 3(c) and 3(d) for ferroelectrics with $g < 0$. Using the numerical values from Tables I and II, we estimated the ranges of dimensionless dynamic parameters as $M^* \sim (0.05\text{–}2)$ and $m^* = (-1.0\text{–}1.5)$ and used the previously determined ranges of static parameters, $0 \leqslant w^* < 1$ for $g > 0$ and $w^* < -2$ for $g < 0$, $-5 < F^* < 5$, $-5 < \alpha_v{}^* < 5$, $0.1 < a^* < 1$, and $-0.5 < k^* < 0.5$ in the first Brillouin zone.

Curves 1–3 in Figs. 3(a) and 3(c) are calculated for fixed α_v^* and several values of flexoconstant F^*, whose signs are different for ferroelectrics with $g > 0$ and $g < 0$ [see the parameters definitions in Table II]. Both O- and A-phonon dispersion curves $\omega^*(k^*)$ are virtually insensitive to F^* values for $k^* \gg 1$. The fact reflects the gradient nature of the flexocoupling. Moreover, O modes are slightly sensitive to the values of F^* for all k^* values. In particular, O modes 1–3 begin to differ very slightly with a k^* increase, and this occurs at $k^* \geqslant 0.1$. In contrast to O mode behavior, A modes are very sensitive to the F^* values at $k^* \geqslant 0.05$. The behavior of A modes 1–3 calculated for different F^* values is principally different for ferroelectrics with $g > 0$ and $g < 0$. The A mode first bends and then disappears with F^* increase at $k^* \geqslant 0.05$ for $g > 0$. For ferroelectrics with $g < 0$, the A mode appears again at $k^* > 0.1$; at that the difference between curves 1–3 decreases. Unlikely, the A mode may appear at $k^* \ll 0.5$ for commensurate ferroelectrics with $g > 0$. However, we cannot state this exactly because the accuracy of the analytical expressions (26) decreases with k^* increase since the higher orders of k^* and its gradients should be considered in the functional (1) for $k^* \ll 0.1$.

Curves 1–3 in Figs. 3(b) and 3(d) are calculated for the fixed value of flexoconstant F^* and several values of reduced

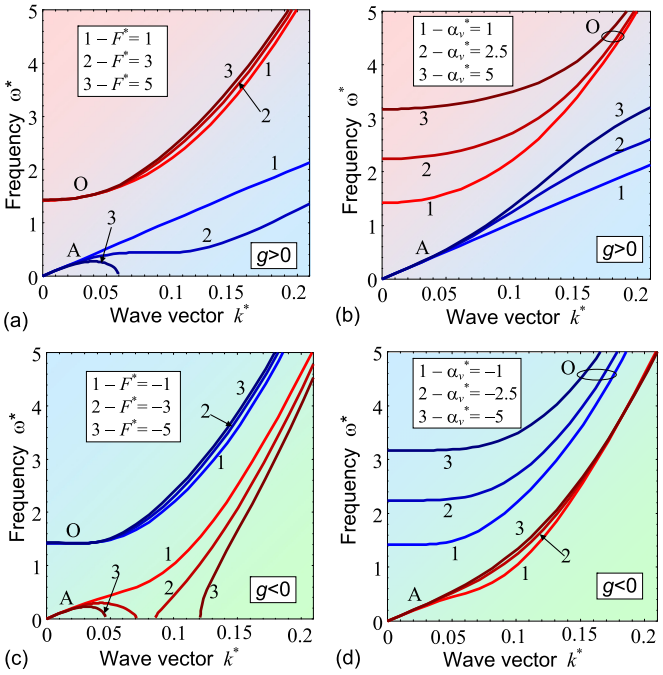

FIG. 3. Dependences of the dimensionless phonon frequency ω^* on the wave vector k^* calculated for ferroelectrics with $g > 0$ (a), (b) and $g < 0$ (c), (d). Curves 1–3 in plots (a), (c) are calculated for $\alpha_v^* = 1$ and several flexoconstants $F^* = 1, 3, 5$ for ferroelectrics with $g > 0$ [plot (a)], and $\alpha_v^* = -1$ and $F^* = -1, -3, -5$ for ferroelectrics with $g < 0$ [plot (c)]. Curves 1–3 in plots (b), (d) are calculated for several values of reduced temperature $\alpha_v^* = 1, 2.5, 5$ and $F^* = 1$ for ferroelectrics with $g > 0$ [plot (b)], $\alpha_v^* = -1, -2.5, -5$ and $F^* = -1$ for ferroelectrics with $g < 0$ [plot (d)], as indicated by legends on the plots. Parameters $Q^* = 0.5$, $M^* = 0.05$, $a^* = 0.1$, $w^* = -2$, and $\mu^* = -1$ for ferroelectrics with $g < 0$; $w^* = 0$ and $\mu^* = 1$ for ferroelectrics with $g > 0$.

temperature α_v^*, whose signs are different for commensurate and incommensurate ferroelectrics with $g > 0$ and $g < 0$, respectively [see the dimensionless parameters definitions in Table II]. For wave vectors $k^* < 0.15$, the O modes are rather sensitive to the values of α_v^* because soft phonons should be sensitive to the temperature changes especially in the vicinity of the ferroelectric phase transition [see curves 1–3 in Figs. 3(b) and 3(d) and compare the values of $\omega^*(0)$ for O modes]. The A modes (curves 1–3) calculated for different α_v^* values become different with k^* increasing for ferroelectrics with $g > 0$ and $g < 0$ [see curves 1–3 in Fig. 3 for A modes]. The A modes calculated for ferroelectrics with $g > 0$ at different α_v^* begin to diverge at wave vectors $k^* \geqslant 0.1$. The A modes calculated for ferroelectrics with $g < 0$ are slightly sensitive to α_v^* values in the region of wave vectors $0.05 \leqslant k^* \leqslant 0.15$ and insensitive outside it.

Our results obtained in the simplest 1D scalar approximation demonstrate that the nontrivial differences in the optical and acoustic phonon dispersion appeared with the flexocoupling constant increase. This is so phonon spectra can give the important information about influence of the flexocoupling on the SMP in ferroelectrics with different signs of the polarization gradient coefficient.

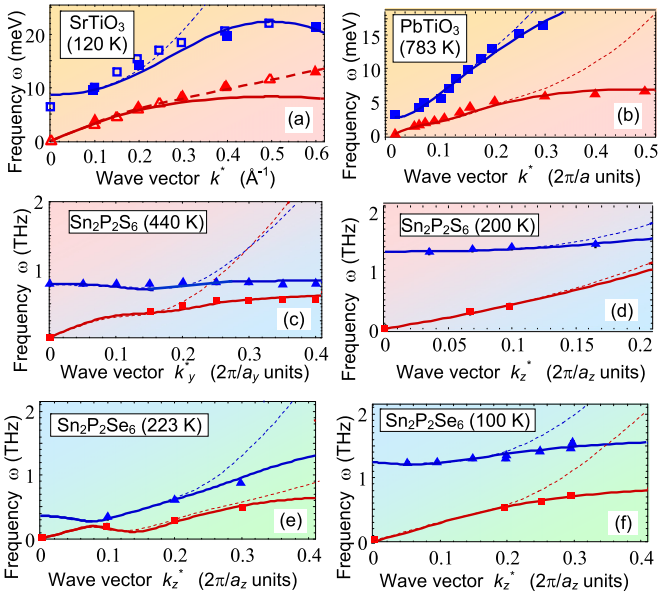

FIG. 4. Dependences of the phonon frequency ω on the wave vector k measured experimentally (symbols) and calculated theoretically (solid and dashed curves) for the lowest transverse optical and acoustic modes in $SrTiO_3$ (a), in the paraelectric phase of $PbTiO_3$ (b), in the paraelectric (c) and ferroelectric (d) phases of $Sn_2P_2S_6$, and in the paraelectric (e) and ferroelectric (f) phases $Sn_2P_2Se_6$. Experimental data are taken from Refs. [43,44,61,62]. Temperatures are specified in plots (a)–(f). Parameters used in our calculations are listed in Table I. Solid and dashed curves were calculated with and without lattice discreteness, respectively.

VI. SOFT PHONON DISPERSION: COMPARISON WITH EXPERIMENT

Since our results are obtained in the simplest 1D scalar approximation, for which the phonon spectrum contains only one acoustic and one optical mode, they cannot describe the interaction between different phonon modes. In particular, the scalar theory cannot describe the interaction between transverse optical, longitudinal, and transverse acoustic modes induced by cooperative effects, flexoelectric, and electrostriction couplings in the ferroelectric phase of multiaxial ferroelectrics [55–57]. That is why we performed quantitative comparison between the calculated and experimentally observed phonon spectra in the uniaxial ferroelectrics $Sn_2P_2S_6$ and $Sn_2P_2Se_6$ [61,62], in which material parameters are relatively well known [58–60]. Unexpectedly, we determined that the scalar theory could describe semiquantitatively the soft phonon dispersion in the incipient ferroelectric $SrTiO_3$ [43], as well as in the paraelectric phase of multiaxial ferroelectric $PbTiO_3$ [44], wherein the interaction between different phonon modes appeared relatively small.

The dependences of the phonon frequency ω on the wave vector k measured experimentally (symbols) and calculated theoretically from Eq. (23) (solid and dashed curves) for the lowest optical and acoustic modes in the incipient ferroelectric $SrTiO_3$ and in the paraelectric phase of commensurate ferroelectrics $PbTiO_3$ are shown in Figs. 4(a) and 4(b), respectively. Experimental data are taken from Shirane and Yamada and

Shirane *et al.* [43,44]. Observed and calculated phonon spectra corresponding to the paraelectric and ferroelectric phases of commensurate ferroelectric $Sn_2P_2S_6$ are shown in Figs. 4(c) and 4(d), respectively. Experimental data are taken from Eijt *et al.* [61]. Phonon spectra corresponding to the paraelectric and ferroelectric phase of $Sn_2P_2Se_6$ are shown in Figs. 4(e) and 4(f), respectively. Experimental data are taken from Eijt *et al.* [62]. Note that the incommensurate phase region is located near T_C in $Sn_2P_2Se_6$.

All material parameters used in our calculations are listed in Table I. The values of $T_C, T_q, \alpha_T, \beta, \gamma, c, q, g, w$, and ρ have been collected from literature. The values of *f, M, v*, and μ are fitting parameters, as their exact or approximate values are unknown. $SrTiO_3$ parameters were collected from Refs. [70–73], $PbTiO_3$ parameters were taken from Refs. [74] and [55], and $Sn_2P_2S_6$ and $Sn_2P_2Se_6$ parameters are collected from Refs. [60–62] and [67–69]. Since we consider only the lowest O and A modes, which are not affected by the depolarization effects, and the wave vector direction $\vec{k} \uparrow\uparrow z$, the anisotropic properties of the elastic, electrostriction, and flexoelectric tensors can be partially accounted by the substitution $c = c_{44}$, $q = q_{44}$, $g = g_{44}$, and $f = f_{44}$. The substitution is valid for materials with cubic m3m parent phase symmetry (such as $SrTiO_3$, $PbTiO_3$, and $BaTiO_3$). For the materials with the lower symmetry of parent phase (such as $Sn_2P_2S_6$ and $Sn_2P_2Se_6$), the values of the c_{44} and c_{55}, q_{44} and q_{55} can be different in a general case. For the case, the elastic constant c and electrostriction coefficient q can be unambiguously determined from the tilt coefficient of the A mode at small $k^* \to 0$. The tilt is equal to $\sqrt{c/\rho}$ in a paraelectric phase and to $\sqrt{(\alpha_S c - 4q^2 P_S^2)/\alpha_S \rho}$ in a ferroelectric one. The gradient coefficients g and w should be determined from the domain wall width. Rigorously speaking, the values *c, q, g*, and w can be regarded as the secondary fitting parameters, but in contrast to the primary fitting parameters *f, M, v*, and μ, the approximate values of *c, q, g*, and w are relatively well known.

It appeared that the fitting parameters *f, M, v*, and μ vary in the ranges $|f| \sim (1-2)\,\mathrm{V}$, $|M| \sim (1-25) \times 10^{-8}\,\mathrm{Vs^2/m^2}$, $v \sim (1-15) \times 10^{-9}\,\mathrm{Vs^2/m^2}$, and $\mu \sim (1.5-25) \times 10^{-18}\mathrm{s^2mJ}$. Since we regard that $f \cong f_{44}$, its range $(1-2)\,\mathrm{V}$ determined from the phonon dispersion is in a perfect agreement with the experiments performed by Zubko *et al.* [72,73] and microscopic estimates made by Kogan [3]. Moreover the result $f \sim (1-2)\,\mathrm{V}$ is in a reasonable agreement with the difference of the values $(f_{11} - f_{12})/2 \sim f_{44}$ calculated from the *ab initio* approach by Hong and Vanderbilt [30,32], Ponomareva *et al.* [31], and Stengel [33,41]. We obtained that the product fM is positive, so both of the fitting parameters should be positive or negative simultaneously. Relatively high values of $M \sim 25 \times 10^{-8}\,\mathrm{Vs^2/m^2}$ estimated for $SrTiO_3$ probably require independent verification.

Solid and dashed curves were calculated with and without lattice discreteness, respectively. Since dashed and solid curves are in a quantitative agreement with experimental data at least for $k^* \leqslant 0.25$, extracted values of the fitting parameters *f, M, v*, and μ seem reliable. Our fitting procedure proves the importance of the static, and dynamic flexoeffect, and the squire of elastic strain gradient (v term) for the quantitative description of available experimental data. For instance, we previously fit the scattering data in $PbTiO_3$ without the v term and consider anisotropic properties of the material tensors (see Fig. 4 in Ref. [55]). This paper shows that the v term allows us to expand the region of the theory and experiment coincidence up to $k^* \leqslant 0.3$ for the A mode and up to $k^* \leqslant 0.5$ for the O mode, respectively [compare solid curves and experimental points in Fig. 4(b)]. Since we consider only one optical mode, rigorous agreement with experiment at wave numbers $k^* > 0.25$ is possible taking into account other optical modes.

VII. SUMMARY

Within the framework of LGD theory, we studied the role of the flexocoupling between the order parameter and elastic strain gradients in the stability of SPM phases in ferroics (such as incipient ferroelectrics and uniaxial ferroelectrics with commensurate and incommensurate phases of the long-range order parameter). Our free energy includes the square of elastic strain gradient that is mandatorily required for the system stability. Performed analysis showed that the fundamental upper limits for the magnitude of the static flexoelectric coefficients established by Yudin, Ahluwalia, and Tagantsev [37] without the square of elastic strain gradient should be substituted by the temperature dependent condition on the flexoelectric coupling strength.

Moreover, the condition is required for the SPM phase appearance in ferroelectrics with the higher gradients of the order parameter. Also, we established that the SMP appears and becomes stable in uniaxial ferroelectrics with positive polarization gradient coefficient g once the flexocoupling constant f exceeds the critical value f_{cr}, which increases with the temperature increase. For smaller f, the phase with homogeneous ferroelectric polarization is absolutely stable. The phase diagram of ferroelectrics with $g < 0$ appeared more complex than the one for ferroelectrics with $g > 0$. For ferroelectrics with $g < 0$, the SMP exists at zero f until the value of α_v is less that the critical one, $\alpha < \alpha_{cr}$. When $\alpha_v > \alpha_{cr}$, the critical value f_{cr} appears and increases with α_v increase. Obtained analytical expressions show that f_{cr} is defined by the reduced temperature, strain and order parameter gradients, electrostriction constant, and expansion coefficients in the LGD functional.

We derived analytical expressions for two modulation wave vectors k_- and k_+ in the SMP and analyzed their dependences on parameters f and α_v. Then, we calculated the soft phonon frequency dispersion, $\omega(k)$, for uniaxial ferroelectrics with different signs of the polarization gradient coefficient, allowing for the square of elastic strain gradient, static and dynamic flexocoupling, and higher order gradient of the order parameter. It appeared that $\omega(k)$ for the optical mode is slightly sensitive to the flexocoupling, and $\omega(k)$ for acoustic mode strongly depends on the coupling strength. Thus, our results in the simplest 1D scalar approximation (one acoustic and one optical mode are considered) demonstrate the appearance of nontrivial differences in the dispersion of optical and acoustic modes with the flexocoupling constants increase. Hence, the phonon spectra analysis can give the important information about the influence of the flexocoupling on the SMP in various ferroelectrics.

Finally, we would like to underline that the criteria of Ref. [37] should be modified not only in the case of higher order gradient terms inclusion in the free energy but also whenever additional optical degrees of freedom are considered. This case is realized in multiaxial ferroelectric perovskites, wherein three acoustic and several optical phonon modes are observed. In this case, the coupling between different phonon modes can either act cooperatively with the flexocoupling or against it [56,57]. Unfortunately the analytical expressions for phonon dispersion law are absent in the anisotropic case with higher order gradient terms in the free energy. We hope that the challenging task will be solved in near future.

ACKNOWLEDGMENTS

Authors express deep gratitude to the Referees. A.N.M. and E.A.E. acknowledge the National Academy of Sciences of Ukraine (Grant No. 07-06-15) and the Center for Nanophase Materials Sciences (Grant No. CNMS2016-061).

APPENDIX: TENSOR FORM OF THE LGD FREE ENERGY AND LAGRANGE FUNCTION

The bulk part of LGD free energy F has the form,

$$F = \int_V d^3r \begin{pmatrix} \frac{a_{ij}(T)}{2} P_i P_j + \frac{a_{ijkl}}{4} P_i P_j P_k P_l + \frac{a_{ijklmn}}{6} P_i P_j P_k P_l P_m P_n - \eta_i \left(E_{0i} + \frac{E_i^d}{2} \right) \\ + \frac{g_{ijkl}}{2} \left(\frac{\partial P_i}{\partial x_j} \frac{\partial P_k}{\partial x_l} \right) + \frac{w_{ijkl}}{2} \left(\frac{\partial^2 P_i}{\partial x_j^2} \frac{\partial^2 P_k}{\partial x_l^2} \right) + \frac{h_{ijk}}{2} \cdot P_i^2 \left(\frac{\partial P_j}{\partial x_k} \right)^2 \\ - \frac{f_{ijkl}}{2} \left(P_k \frac{\partial u_{ij}}{\partial x_l} - u_{ij} \frac{\partial P_k}{\partial x_l} \right) - q_{ijkl} u_{ij} P_k P_l + \frac{c_{ijkl}}{2} u_{ij} u_{kl} + \frac{v_{ijklmn}}{2} \left(\frac{\partial u_{ij}}{\partial x_m} \frac{\partial u_{kl}}{\partial x_n} \right) \end{pmatrix}. \tag{A1}$$

The values P_i are the components of ferroelectric polarization vector (order parameter); u_{ij} are the components of the strain tensor. In many cases, one could suppose that coefficients $a_{ij}(T) = \alpha_{ij}^T (T - T_C)$ linearly depend on temperature T, but in some cases Barrett-type [65] formula $a_{ij} = \alpha_{ij}^T (T_q \coth(T_q/T) - T_C)$ should be used. Note that for proper ferroelectrics, $T_C > T_q$, while $T_C < T_q$ for the incipient ones. T_C is the Curie temperature, and T_q is a characteristic temperature, which is sometimes called the temperature of quantum vibrations. Coefficients a_{ij}, a_{ijkl}, and a_{ijklmn} are supposed to be temperature independent; tensors g_{ijkl}, w_{ijkl}, and v_{ijklmn} determine the magnitude of the gradient energy. Tensors v_{ijklmn}, w_{ijkl}, and a_{ijkl} are positively defined; q_{ijkl} are the components of electrostriction tensor; and c_{ijkl} are the components of elastic stiffness tensor. The order parameter is conjugated with depolarization field E_i^d (if any exists). External field is E_{0i}. The Lifshitz invariant is $\frac{f_{ijkl}}{2}(P_k \frac{\partial u_{ij}}{\partial x_l} - u_{ij} \frac{\partial P_k}{\partial x_l})$; tensor f_{ijkl} is the flexocoupling coefficient tensor.

Lagrange function is

$$L = \int_t dt (F - K), \tag{A2}$$

where the kinetic energy K is given by expression

$$K = \int_V d^3r \left(\frac{\mu}{2} \left(\frac{\partial P_i}{\partial t} \right)^2 + M_{ij} \frac{\partial P_i}{\partial t} \frac{\partial U_j}{\partial t} + \frac{\rho}{2} \left(\frac{\partial P_i}{\partial t} \right)^2 \right), \tag{A3}$$

which includes the dynamic flexoelectric coupling tensor M_{ij}. U_i is the elastic displacement, and ρ is the density of a material. The strain components $u_{ij} = \frac{1}{2}(\frac{\partial U_i}{\partial x_j} + \frac{\partial U_j}{\partial x_i})$.

Dynamic equations of state have the form of Euler-Lagrange equations allowing for the possible Khalatnikov-type relaxation of the polarization,

$$\Gamma \frac{\partial P_i}{\partial t} = -\frac{\delta L}{\delta P_i}, \frac{\delta L}{\delta U_i} = 0. \tag{A4}$$

[1] A. K. Tagantsev, Piezoelectricity and flexoelectricity in crystalline dielectrics, Phys. Rev. B **34**, 5883 (1986).
[2] V. S. Mashkevich and K. B. Tolpygo, The interaction of vibrations of nonpolar crystals with electric fields, Zh. Eksp. Teor. Fiz. **31**, 520 (1957).
[3] Sh. M. Kogan, Piezoelectric effect under an inhomogeneous strain and an acoustic scattering of carriers of current in crystals, Solid State Phys. **5**, 2829 (1963).
[4] J. D. Axe, J. Harada, and G. Shirane, Anomalous acoustic dispersion in centrosymmetric crystals with soft optic phonons, Phys. Rev. B **1**, 1227 (1970).
[5] P. V. Yudin and A. K. Tagantsev, Fundamentals of flexoelectricity in solids, Nanotechnology **24**, 432001 (2013).
[6] A. Kvasov and A. K. Tagantsev, Dynamic flexoelectric effect in perovskites from first-principles calculations, Phys. Rev. B **92**, 054104 (2015).
[7] P. Zubko, G. Catalan, and A. K. Tagantsev, Flexoelectric effect in solids, Annu. Rev. Mater. Res. **43**, 387 (2013).
[8] M. Fiebig, Revival of the magnetoelectric effect, J. Phys. D: Appl. Phys. **38**, R123 (2005).
[9] A. S. Zimmermann, D. Meier, and M. Fiebig, Ferroic nature of magnetic toroidal order, Nat. Comm. **5**, 4796 (2014).

[10] M. Lilienblum, T. Lottermoser, S. Manz, S. M. Selbach, A. Cano, and M. Fiebig, Ferroelectricity in the multiferroic hexagonal manganites, Nat. Phys. **11**, 1070 (2015).
[11] S. V. Kalinin and A. N. Morozovska, Multiferroics: Focusing the light on flexoelectricity, Nat. Nanotechnol. **10**, 916 (2015).
[12] G. Catalan, L. J. Sinnamon, and J. M. Gregg, The effect of flexoelectricity on the dielectric properties of inhomogeneously strained ferroelectric thin films, J. Phys.: Condens. Matter **16**, 2253 (2004).
[13] G. Catalan, B. Noheda, J. McAneney, L. J. Sinnamon, and J. M. Gregg, Strain gradients in epitaxial ferroelectrics, Phys. Rev. B **72**, 020102 (2005).
[14] M. S. Majdoub, R. Maranganti, and P. Sharma, Understanding the origins of the intrinsic dead layer effect in nanocapacitors, Phys. Rev. B **79**, 115412 (2009).
[15] H. Zhou, J. Hong, Y. Zhang, F. Li, Y. Pei, and D. Fang, Flexoelectricity induced increase of critical thickness in epitaxial ferroelectric thin films, Physica B (Amsterdam, Neth.) **407**, 3377 (2012).
[16] E. A. Eliseev, A. N. Morozovska, M. D. Glinchuk, and R. Blinc, Spontaneous flexoelectric/flexomagnetic effect in nanoferroics, Phys. Rev. B **79**, 165433 (2009).
[17] E. A. Eliseev, M. D. Glinchuk, V. Khist, V. V. Skorokhod, R. Blinc, and A. N. Morozovska, Linear magnetoelectric coupling and ferroelectricity induced by the flexomagnetic effect in ferroics, Phys. Rev. B **84**, 174112 (2011).
[18] A. Kholkin, I. Bdikin, T. Ostapchuk, and J. Petzelt, Room temperature surface piezoelectricity in $SrTiO_3$ ceramics via piezoresponse force microscopy, Appl. Phys. Lett. **93**, 222905 (2008).
[19] R. Tararam, I. K. Bdikin, N. Panwar, J. Arana Varela, P. R. Bueno, and A. L. Kholkin, Nanoscale electromechanical properties of $CaCu_3Ti_4O_{12}$ ceramics, J. Appl. Phys. **110**, 052019 (2011).
[20] E. A. Eliseev, A. N. Morozovska, G. S. Svechnikov, P. Maksymovych, and S. V. Kalinin, Domain wall conduction in multiaxial ferroelectrics: Impact of the wall tilt, curvature, flexoelectric coupling, electrostriction, proximity and finite size effects, Phys. Rev. B **85**, 045312 (2012).
[21] P. V. Yudin, A. K. Tagantsev, E. A. Eliseev, A. N. Morozovska, and N. Setter, Bichiral structure of ferroelectric domain walls driven by flexoelectricity, Phys. Rev. B **86**, 134102 (2012).
[22] Y. Gu, M. Li, A. N. Morozovska, Y. Wang, E. A. Eliseev, V. Gopalan, and L.-Q. Chen, Non-Ising character of a ferroelectric wall arises from a flexoelectric effect, Phys. Rev. B **89**, 174111 (2014).
[23] E. A. Eliseev, P. V. Yudin, S. V. Kalinin, N. Setter, A. K. Tagantsev, and A. N. Morozovska, Structural phase transitions and electronic phenomena at 180-degree domain walls in rhombohedral $BaTiO_3$, Phys. Rev. B **87**, 054111 (2013).
[24] A. N. Morozovska, E. A. Eliseev, M. D. Glinchuk, L.-Q. Chen, and V. Gopalan, Interfacial polarization and pyroelectricity in antiferrodistortive structures induced by a flexoelectric effect and rotostriction, Phys. Rev. B **85**, 094107 (2012).
[25] E. A. Eliseev, A. N. Morozovska, Y. Gu, A. Y. Borisevich, L.-Q. Chen, V. Gopalan, and S. V. Kalinin, Conductivity of twin walls - surface junctions in ferroelastics: Interplay of deformation potential, octahedral rotations, improper ferroelectricity and flexoelectric coupling, Phys. Rev. B **86**, 085416 (2012).
[26] A. N. Morozovska and M. D. Glinchuk, Reentrant phase in nanoferroics induced by the flexoelectric and Vegard effects, J. Appl. Phys. **119**, 094109 (2016).
[27] A. Y. Borisevich, E. A. Eliseev, A. N. Morozovska, C.-J. Cheng, J.-Y. Lin, Y.-H. Chu, D. Kan, I. Takeuchi, V. Nagarajan, and S. V. Kalinin, Atomic-scale evolution of modulated phases at the ferroelectric–antiferroelectric morphotropic phase boundary controlled by flexoelectric interaction, Nat. Commun. **3**, 775 (2012).
[28] E. A. Eliseev, S. V. Kalinin, Y. Gu, M. D. Glinchuk, V. V. Khist, A. Y. Borisevich, V. Gopalan, L.-Q. Chen, and A. N. Morozovska, Universal emergence of spatially-modulated structures induced by flexo-antiferrodistortive coupling in multiferroics, Phys. Rev. B **88**, 224105 (2013).
[29] H. Pöttker and E. K. H. Salje, Flexoelectricity, incommensurate phases and the Lifshitz point, J. Phys.: Condens. Matter **28**, 075902 (2016).
[30] J. Hong and D. Vanderbilt, First-principles theory of frozen-ion flexoelectricity, Phys. Rev. B **84**, 180101(R) (2011).
[31] I. Ponomareva, A. K. Tagantsev, and L. Bellaiche, Finite-temperature flexoelectricity in ferroelectric thin films from first principles, Phys. Rev. B **85**, 104101 (2012).
[32] J. Hong and D. Vanderbilt, First-principles theory and calculation of flexoelectricity, Phys. Rev. B **88**, 174107 (2013).
[33] M. Stengel, Flexoelectricity from density-functional perturbation theory, Phys. Rev. B **88**, 174106 (2013).
[34] W. Ma and L. E. Cross, Strain-gradient-induced electric polarization in lead zirconate titanate ceramics, Appl. Phys. Lett. **82**, 3293 (2003).
[35] W. Ma and L. E. Cross, Flexoelectricity of barium titanate, Appl. Phys. Lett. **88**, 232902 (2006).
[36] W. Ma and L. E. Cross, Flexoelectric effect in ceramic lead zirconate titanate, Appl. Phys. Lett. **86**, 072905 (2005).
[37] P. V. Yudin, R. Ahluwalia, and A. K. Tagantsev, Upper bounds for flexocoupling coefficients in ferroelectrics, Appl. Phys. Lett. **104**, 082913 (2014).
[38] A. P. Levanyuk and D. G. Sannikov, Thermodynamic theory of phase transitions accompanied by the formation of the noncommensurate superstructure in $NaNO_2$, Sov. Phys. Sol. St. **18**, 1122 (1976).
[39] A. S. Yurkov, Elastic boundary conditions in the presence of the flexoelectric effect, JETP Lett. **94**, 455 (2011).
[40] S. Mao and P. K. Purohit, Insights into flexoelectric solids from strain-gradient elasticity, J. Appl. Mech. **81**, 081004 (2014).
[41] M. Stengel, Unified ab initio formulation of flexoelectricity and strain-gradient elasticity, Phys. Rev. B **93**, 245107 (2016).
[42] W. Cochran, Dynamical, scattering and dielectric properties of ferroelectric crystals, Adv. Phys. **18**, 157 (1969).
[43] G. Shirane and Y. Yamada, Lattice-dynamical study of the 110° K phase transition in $SrTiO_3$, Phys. Rev. **177**, 858 (1969).
[44] G. Shirane, J. D. Axe, J. Harada, and J. P. Remeika, Soft ferroelectric modes in lead titanate, Phys. Rev. B **2**, 155 (1970).
[45] R. Currat, H. Buhay, C. H. Perry, and A. M. Quittet, Inelastic neutron scattering study of anharmonic interactions in orthorhombic $KNbO_3$, Phys. Rev. B **40**, 10741 (1989).
[46] I. Etxebarria, M. Quilichini, J. M. Perez-Mato, P. Boutrouille, F. J. Zuniga, and T. Breczewski, Inelastic neutron scattering investigation of external modes in incommensurate and commensurate A_2BX_4 materials, J. Phys.: Condens. Matter **4**, 8551 (1992).

[47] J. Hlinka, M. Quilichini, R. Currat, and J. F. Legrand, Dynamical properties of the normal phase of betaine calcium chloride dihydrate. I. Experimental results, J. Phys.: Condens. Matter **8**, 8207 (1996).

[48] J. Hlinka, S. Kamba, J. Petzelt, J. Kulda, C. A. Randall, and S. J. Zhang, Origin of the "Waterfall" Effect in Phonon Dispersion of Relaxor Perovskites, Phys. Rev. Lett. **91**, 107602 (2003).

[49] V. Goian, S. Kamba, O. Pacherova, J. Drahokoupil, L. Palatinus, M. Dusek, J. Rohlıcek, M. Savinov, F. Laufek, W. Schranz, A. Fuith, M. Kachlık, K. Maca, A. Shkabko, L. Sagarna, A. Weidenkaff, and A. A. Belik, Antiferrodistortive phase transition in $EuTiO_3$, Phys. Rev. B **86**, 054112 (2012).

[50] A. K. Tagantsev, K. Vaideeswaran, S. B. Vakhrushev, A. V. Filimonov, R. G. Burkovsky, A. Shaganov, D. Andronikova, A. I. Rudskoy, A. Q. R. Baron, H. Uchiyama, D. Chernyshov, A. Bosak, Z. Ujma, K. Roleder, A. Majchrowski, J.-H. Ko, and N. Setter, The origin of antiferroelectricity in $PbZrO_3$, Nat. Commun. **4**, 2229 (2013).

[51] J.-W. Kim, P. Thompson, S. Brown, P. S. Normile, J. A. Schlueter, A. Shkabko, A. Weidenkaff, and P. J. Ryan, Emergent Superstructural Dynamic Order due to Competing Antiferroelectric and Antiferrodistortive Instabilities in Bulk $EuTiO_3$, Phys. Rev. Lett. **110**, 027201 (2013).

[52] R. G. Burkovsky, A. K. Tagantsev, K. Vaideeswaran, N. Setter, S. B. Vakhrushev, A. V. Filimonov, A. Shaganov, D. Andronikova, A. I. Rudskoy, A. Q. R. Baron, H. Uchiyama, D. Chernyshov, Z. Ujma, K. Roleder, A. Majchrowski, and J.-H. Ko, Lattice dynamics and antiferroelectricity in $PbZrO_3$ tested by x-ray and Brillouin light scattering, Phys. Rev. B **90**, 144301 (2014).

[53] J. Hlinka, I. Gregora, and V. Vorlıcek, Complete spectrum of long-wavelength phonon modes in $Sn_2P_2S_6$ by Raman scattering, Phys. Rev. B **65**, 064308 (2002).

[54] A. Kohutych, R. Yevych, S. Perechinskii, V. Samulionis, J. Banys, and Yu. Vysochanskii, Sound behavior near the Lifshitz point in proper ferroelectrics, Phys. Rev. B **82**, 054101 (2010).

[55] A. N. Morozovska, Yu. M. Vysochanskii, O. V. Varenik, M. V. Silibin, S. V. Kalinin, and E. A. Eliseev, Flexocoupling impact on the generalized susceptibility and soft phonon modes in the ordered phase of ferroics, Phys. Rev. B **92**, 094308 (2015).

[56] C. Kappler and M. B. Walker, Symmetry-based model for the modulated phases of betaine calcium chloride dihydrate, Phys. Rev. B **48**, 5902 (1993).

[57] J. Hlinka, M. Quilichini, R. Currat, and J. F. Legrand, Dynamical properties of the normal phase of betaine calcium chloride dihydrate. II. A semimicroscopic model, J. Phys.: Condens. Matter **8**, 8221 (1996).

[58] Yu. M. Vysochanskii, M. M. Mayor, V. M. Rizak, V. Yu. Slivka, and M. M. Khoma, The tricritical Lifshitz point on the phase diagram of $Sn_2P_2(Se_xS_{1-x})_6$ ferroelectrics, Zh. Eksp. Teor. Fiz. **95**, 1355 (1989) [Sov. Phys. JETP **68**, 782 (1989)].

[59] M. M. Khoma, A. A. Molnar, and Yu. M. Vysochanskii, The mean field analysis of $Sn_2P_2(Se_xS_{1-x})_6$ thermodynamical properties in the paraelectric, incommensurate and ferroelectric phases, J. Phys. Studies **2**, 524 (1998).

[60] R. M. Yevych, Yu. M. Vysochanskii, M. M. Khoma, and S. I. Perechinskii, Lattice instability at phase transitions near the Lifshitz point in proper monoclinic ferroelectrics, J. Phys.: Condens. Matter **18**, 4047 (2006).

[61] S. W. H. Eijt, R. Currat, J. E. Lorenzo, P. Saint-Gregoire, B. Hennion, and Yu. M. Vysochanskii, Soft modes and phonon interactions in $Sn_2P_2S_6$ studied by neutron scattering, Eur. Phys. J. B **5**, 169 (1998).

[62] S. W. H. Eijt, R. Currat, J. E. Lorenzo, P. Saint-Gregoire, S. Katano, T. Janssen, B. Hennion, and Yu. M. Vysochanskii, Soft modes and phonon interactions in $Sn_2P_2Se_6$ studied by means of neutron scattering, J. Phys.: Condens. Matter **10**, 4811 (1998).

[63] L. D. Landau and E. M. Lifshitz, *Theory of Elasticity. Theoretical Physics*, Vol. 7 (Butterworth-Heinemann, Oxford, U.K.,1998).

[64] G. A. Smolenskii, V. A. Bokov, V. A. Isupov, N. N Krainik, R. E. Pasynkov, and A. I. Sokolov, *Ferroelectrics and Related Materials* (Gordon and Breach, New York, 1984).

[65] J. H. Barrett, Dielectric constant in perovskite type crystals, Phys. Rev. **86**, 118 (1952).

[66] A. N. Morozovska, E. A. Eliseev, J. J. Wang, G. S. Svechnikov, Y. M. Vysochanskii, V. Gopalan, and L.-Q. Chen, Phase diagrams and domain splitting in thin ferroelectric films with incommensurate phases, Phys. Rev. B **81**, 195437 (2010).

[67] A. A. Kohutych, R. M. Yevych, S. I. Perechinskii, and Y. M. Vysochanskii, Acoustic attenuation in ferroelectric $Sn_2P_2S_6$ crystals, Open Physics **8**, 905 (2010).

[68] O. Mys, I. Martynyuk-Lototska, A. Grabar, and R. Vlokh, Acoustic and elastic properties of $Sn_2P_2S_6$ crystals, J. Phys.: Condens. Matter **21**, 265401 (2009).

[69] V. M. Rizak, I. M. Rizak, S. I. Perechinskii, Yu. M. Vysochanskii, and V. Yu. Slivka, Effect of uniaxial compression on phase transitions in $Sn_2P_2S_6$-type ferroelectrics, Phys. Stat. Sol. (b) **183**, 97 (1994).

[70] N. A. Pertsev, A. K. Tagantsev, and N. Setter, Phase transitions and strain-induced ferroelectricity in $SrTiO_3$ epitaxial thin films, Phys. Rev. B **61**, R825 (2000).

[71] A. K. Tagantsev, E. Courtens, and L. Arzel, Prediction of a low-temperature ferroelectric instability in antiphase domain boundaries of strontium titanate, Phys. Rev. B **64**, 224107 (2001).

[72] P. Zubko, G. Catalan, A. Buckley, P. R. L. Welche, and J. F. Scott, Strain-Gradient-Induced Polarization in $SrTiO_3$ Single Crystals, Phys. Rev. Lett. **99**, 167601 (2007).

[73] P. Zubko, G. Catalan, A. Buckley, P. R. L. Welche, and J. F. Scott, Erratum: Strain-Gradient-Induced Polarization in $SrTiO_3$ Single Crystals [Phys. Rev. Lett. **99**, 167601 (2007)], Phys. Rev. Lett. **100**, 199906 (2008).

[74] M. J. Haun, E. Furman, S. J. Jang, H. A. McKinstry, and L. E. Cross, Thermodynamic theory of $PbTiO_3$, J. Appl. Phys. **62**, 3331 (1987).